is governed through a dynamic balance between the activity of excitation factors (such as kinases) and de-excitation factors (such as phosphatases), the ratio of which defines a threshold for activation. This threshold reflects the summation of previous signals through the TCR as well as other signals received from the cellular environment.

Thus, within the thymus, thymocytes that are positively selected receive signals of increasing avidity from self-peptide–MHC complexes. The signals are of increasing avidity because of the up-regulation of TCR expression during thymocyte development. As the cell is gradually exposed to signals of increasing strength, its threshold for activation also rises such that when a thymocyte matures and emigrates, the self-peptide on which is was selected can no longer provide sufficiently strong signals to perturb the ratio of excitation to de-excitation factors past the activation threshold. Rather, in the periphery, these "sub-threshold" TCR stimulations provided by self-peptide–MHC play a critical role in maintaining the activation threshold such that the T cell will be able to respond quickly when a higher affinity/avidity signal is provided, such as the signal provided by invading pathogens.

Some experimental evidence exists that supports the theory of tunable T cell activation. Studies from our laboratory have demonstrated tuning of thymocytes bearing a defined transgenic TCR. Thymocytes selected upon a certain peptide lose their ability to proliferate to that peptide as mature T cells while still retaining the ability to proliferate to higher affinity peptides. This was demonstrated with cells selected *in vivo* [10] or in fetal thymic organ culture (FTOC) [11, 12].

Other groups have also demonstrated tuning of T cell responsiveness in developing as well as mature cells. Alteration in activation potentials of thymocytes was demonstrated by exposure to peptide–MHC complexes that do not have significant avidity to induce positive selection [13]. As well, effector function and cytokine secretion elicited *in vitro* from mature T cells were demonstrated to be tunable. Selection of a virus-specific TCR in the presence of an antagonist peptide was shown to affect activation and effector function of mature transgenic T cells when challenged with the viral antigen *in vitro* [14]. Also, the cytokine secretion profile from a polyclonal T cell population challenged by the same peptide was shown to be adaptable and modulated by previous exposure to a suboptimal, cross-reactive peptide [15]. All of these findings suggest that the activation threshold of T cells is influenced by previous signals received through the TCR.

In this study we wanted to identify potential self-peptides that could mediate positive selection of a defined, transgenic TCR, P14. Two peptides, DBM and RPP, were shown to mediate positive selection and alter the functional response of mature T cells. These data show for the first time that the peptide RPP can tune thymocyte activation thresholds in a dose-dependent fashion.

2 Results

2.1 Identification and characterization of related peptides

To define potential peptides that could mediate positive selection of a virus-specific TCR, we identified self-peptides that were homologous to the defined viral peptide (KAVYNFATC). This viral peptide, derived from the glycoprotein of the lymphocytic choriomeningitis virus (LCMV), was chosen because it is recognized by the P14 transgenic TCR in the context of H-2D^b. To identify related natural peptides, the SwissPlot protein database was searched using a similar strategy to one that was previously reported [16]. The first search identified a rat peptide (KALYNYAPI) derived from the dopamine β-monooxygenase (rDBM) protein. The sequence of this peptide was used to focus subsequent searches. A second search yielded two more peptides, murine DBM (KALYDYAPI) — henceforth called DBM — and RPP (KAIYRFNAI), that have been previously described [16]. Finally, a third search was conducted for peptides that contained elements common to the three previously identified peptides: lysine at position 1, alanine at position 2 and isoleucine at position 9. This search identified novel peptides HP3 and EGFR. The sequences of all the peptides used in this study and the proteins from which they are derived are summarized in Fig. 1A.

Having identified peptides that bear some homology to the viral peptide p33, we examined whether these peptides could be presented by H-2D^b. Because of their lack of the TAP-2 transporter, RMA-S cells only stably express H-2D^b molecules at their surface when peptides capable of binding this MHC molecule are exogenously added to the cell culture [17]. The amount of H-2D^b expression restored by the various peptides over a range of concentrations is shown in Fig. 1B. DBM, RPP, HP3 and EGFR peptides were capable of binding H-2D^b although only the DBM and RPP peptides were able to rescue H-2D^b expression at lower peptide concentrations.

Previous work has shown that different peptide agonists could induce positive selection of P14 thymocytes [11,

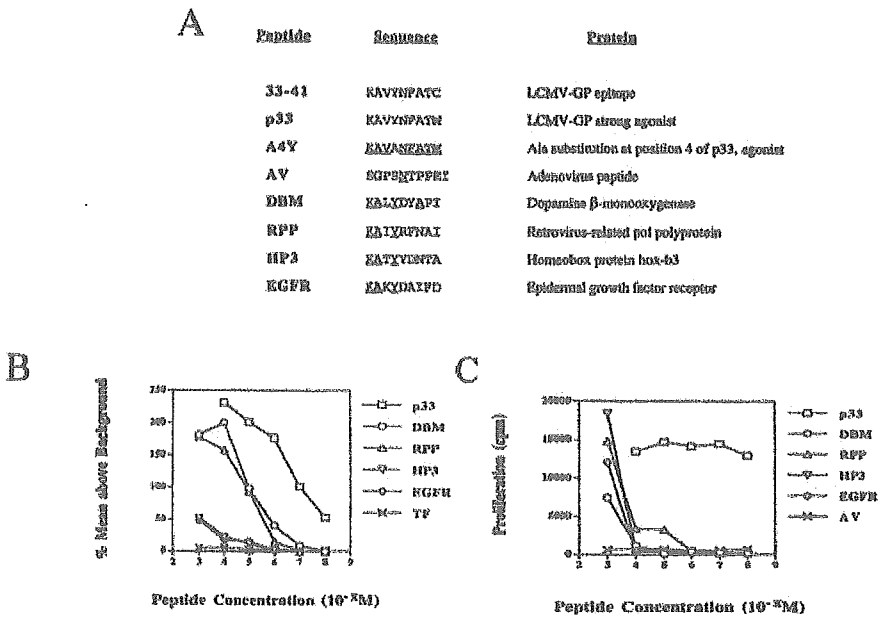

Fig. 1. Description of potential self-peptides involved in positive selection. (A) Natural LCMV peptide sequence in comparison with peptides used in this study: the abbreviation of each peptide, its sequence and the name of the protein are listed, and amino acid homologies are underlined. (B) Peptides bind to the H-2D^b molecule. The relative expression of H-2D^b was monitored on RMA-S cells incubated with various concentrations of different peptides. Peptides that were relevant to this study are shown. TF peptide was used as a negative control. (C) Peptides DBM, EGFR, HP3 and RPP are weak agonist ligands for P14 cells. Spleen cells from P14 TCR transgenic mice were co-cultivated in the presence of different peptides at the concentrations shown. Peptides were added once daily. Proliferation was measured by [^{3}H]thymidine incorporation; cpm, counts per minute. Data are representative of at least four experiments. p33 was used as a positive control and AV as a negative control.

12, 18, 19]. Therefore, the peptides that were able to bind H-2D^b were then tested for their ability to induce proliferation of cells bearing the P14 TCR. Naïve TCR transgenic splenocytes were co-cultured with APC and varying concentrations of peptide, and proliferation was measured. The p33 peptide was used as a positive control, whereas the AV peptide was used for a negative control as it is able to bind H-2D^b but is not recognized by the transgenic TCR. The results of these experiments are shown in Fig. 1C and demonstrate that four peptides (DBM, RPP, HP3 and EGFR) were able to induce proliferation to various degrees. Previous work in our laboratory characterized DBM and RPP peptides as having weak agonist as well as antagonist properties [16].

2.2 Peptides DBM and RPP but not EGFR and HP3 induce positive selection

DBM, RPP, EGFP and HP3 were tested for their ability to induce positive selection of virus-specific thymocytes. Fetal thymic lobes from transgenic (P14 TCR$^+$), β2-microglobulin deficient (β2m$^{-/-}$) animals were co-cultivated with the peptides and exogenous β2m for six days and then stained with anti-CD4, anti-CD8 and antibodies specific for the Vα2 transgene and analyzed by flow cytometry. The A4Y peptide was used as a positive control as it is known to induce positive selection in this system [11] whereas the adenovirus peptide AV was used as the negative control.

Peptides DBM and RPP were able to increase both the percentage (3–4-fold) and absolute cell number (2–5-fold) of single-positive (SP) CD8$^+$ thymocytes expressing the transgenic TCR at 10^{-4} M concentration (Fig. 2A, B). The increase in the number of SP CD8$^+$ thymocytes observed with DBM and RPP was comparable with that found using the A4Y peptide. Conversely, HP3 and EGFR failed to induce an increase in the number of SP CD8$^+$ thymocytes expressing the transgenic TCR. The cell numbers found with HP3 and EGFR were similar to those found with the AV peptide and to cultures to which no peptide was added (data not shown). These data indicated that DBM and RPP were able to induce positive selection of thymocytes bearing the transgenic TCR.

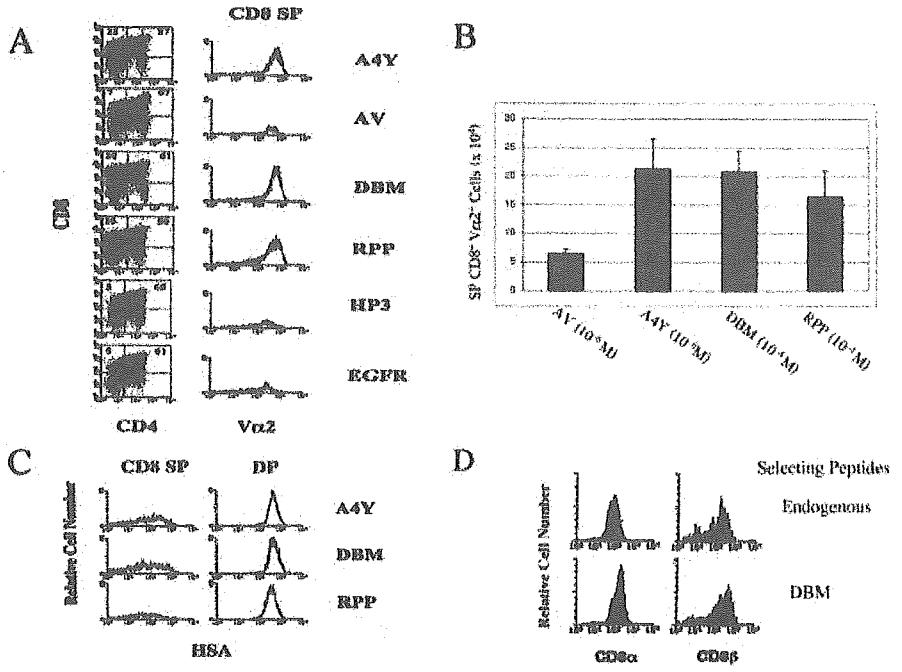

Fig. 2. Two related peptides promote the positive selection of virus-specific T cells. Day 16 fetal thymic lobes from TCR$^+$ β2m$^{-/-}$ mice were co-cultivated with 10^{-4} M peptide in the presence of exogenous β2m for 6 days and analyzed by three-color flow cytometry. Positive and negative control cultures contained A4Y and AV, respectively, both at 10^{-6} M. (A) Cells were stained with anti-CD4, anti-CD8 and anti-Vα2. The Vα2 expression of CD8$^+$ cells is shown. (B) Total numbers of CD8$^+$Vα2$^+$ cells from the peptide-treated FTOC as indicated. (C) Thymocytes were stained for anti-CD4, anti-CD8 and anti-HSA. HSA expression on CD8$^+$ and CD4$^+$CD8$^+$ cells is shown. (D) SP CD8$^+$ thymocytes selected by DBM in FTOC and from P14 transgenic mice were stained with antibodies to CD8α and CD8β. Data are representative of at least three experiments.

To confirm that the thymocytes were mature, cells from DBM-, RPP- or A4Y-treated FTOC were stained for the maturation marker HSA (CD24). All three peptides induced the down-regulation of HSA on SP CD8$^+$ cells compared with the level of HSA expression on the double-positive (DP) cells (Fig. 2C). These data indicated that the DBM and RPP peptides induced positive selection and maturation of P14 thymocytes.

Previous studies [20, 21] have demonstrated that selection of class-I-restricted TCR by agonist ligands can result in the emergence of a CD8^{lo} population that express predominantly CD8α homodimers instead of CD8αβ. These CD8^{lo} cells resemble mature T cells in the expression of other surface markers but are not functional when assayed *in vitro*. To further characterize the phenotype of the thymocytes selected by DBM and RPP, the cells were stained with antibodies for CD8α and CD8β. We found that DBM- and RPP-selected CD8 cells express CD8αβ heterodimers (Fig. 2D, and data not shown). These data, combined with the expression of HSA, demonstrated that the DBM and RPP peptides were able to induce the positive selection of phenotypically normal virus-specific T cells.

2.3 Peptides DBM and RPP do not induce negative selection

Further experiments were done to determine whether DBM or RPP were capable of inducing clonal deletion. Thymic lobes from P14 TCR$^+$, β2m$^{+/+}$ mice were co-cultivated in the presence of either DBM or RPP at 10^{-3} M or 10^{-4} M. As controls, thymic lobes were cultured with either the strong agonist peptide p33 at 10^{-6} M or the nonstimulatory peptide AV at 10^{-6} M. It should be noted that in these assays FTOC were done using lobes from β2m$^+$ mice because there is an increased sensitivity for negative selection in the presence of class I molecules compared with β2m$^{+/-}$ or β2m$^{-/-}$ lobes [22]. Thymocytes were stained with anti-CD4, anti-CD8 and anti-Vα2 and analyzed by flow cytometry.

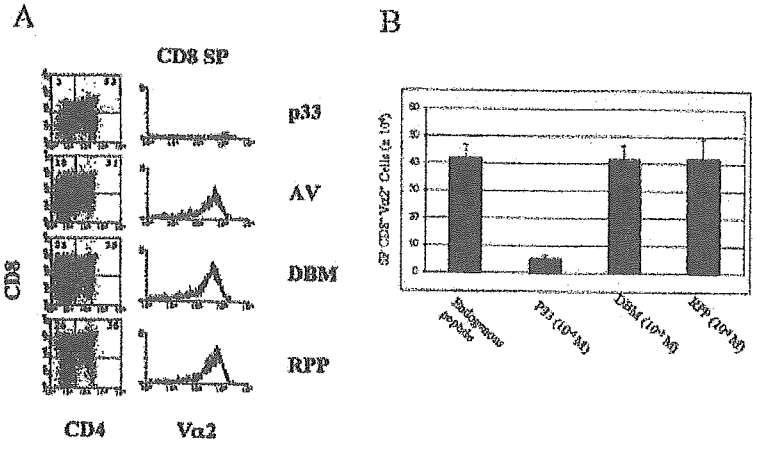

Fig. 3. Clonal deletion is not detected in the presence of positively selecting ligands DBM and RPP. Fetal thymic lobes from TCR$^+$ β2m$^{+/+}$ mice were co-cultivated with 10^{-3} M DBM or RPP peptides for 6 days and then analyzed by three-color flow cytometry. p33 at 10^{-6} M was used as a positive control whereas the AV peptide and endogenous peptides (no peptide added) were used as negative controls. (A) Cells were stained with anti-CD4, anti-CD8 and anti-Vα2. The Vα2 expression of CD8$^+$ cells is shown. (B) Total numbers of CD8$^+$ Vα2$^+$ thymocytes from the peptide-treated FTOC are shown.

The percentage of SP CD8$^+$ transgenic T cells present in the FTOC treated with either DBM or RPP was equivalent to the percentage found in the culture treated with the AV peptide, indicating that clonal deletion did not occur (Fig. 3A). This lack of deletion was further confirmed by the level of expression of Vα2 on the SP CD8$^+$ populations from the DBM- or RPP-treated FTOC, as it was also the same as that observed upon the SP CD8$^+$ population from the AV-treated FTOC. This finding indicates that the SP CD8$^+$ populations from the DBM- or RPP-treated FTOC express normal levels of the P14 transgenic TCR. In contrast, the p33 peptide induced a substantial decrease in the percentage of SP CD8$^+$ cells bearing the transgenic TCR.

Moreover, when the number of SP CD8$^+$ TCR$^+$ cells from each FTOC was counted, it was apparent that p33 led to a dramatic reduction in SP CD8$^+$ TCR$^+$ cell numbers at 10^{-6} M concentration whereas both DBM and RPP failed to induce any detectable deletion at 10^{-4} M and 10^{-3} M (Fig. 3B and data not shown). Taken together, these data indicate that clonal deletion was not induced in FTOC in the presence of the DBM or RPP peptides.

In FTOC treated with AV, DBM or RPP, fewer DP cells were observed compared with the cultures treated with p33. It is likely that this is due to the efficient positive selection of the CD8 cells expressing the transgene, since these FTOC were done with class-I$^+$ lobes. In the FTOC cocultured with p33, the transgenic TCR would have been down-regulated and, therefore, the T cells had to rearrange TCR genes and undergo receptor editing in order to proceed through further selection events in the thymus [23]. It is possible, however, that the presence of the cognate ligand arrests development, as previously reported [24].

2.4 Peptides DBM and RPP are expressed by thymic epithelial cell lines

Since DBM and RPP were able to induce positive selection, we examined whether these peptides could be natural self ligands presented on thymic epithelium. Murine thymic epithelial cell lines that were previously shown to mediate positive selection *in vivo* [25, 26] were analyzed for expression of DBM and RPP by Northern blot.

Five different thymic cell lines including epithelial cell lines (2A9 and 5.1) and the stromal cell line 4.1 expressed both DBM and RPP (Fig. 4, and data not shown). This is perhaps surprising for DBM, which is an enzyme involved in the conversion of dopamine to norepinephrine and is mainly expressed in the adrenal gland and adrenergic neurons [27]. It is, however, less surprising for RPP, which encodes a retrovirus-related polyprotein that is highly conserved in the murine genome. RPP is encoded within a mobile DNA element of which between 10,000 and 85,000 copies are present within the genome [28]. Furthermore, the promoter region of the RPP gene shares homology with several house-keeping genes, which results in its ubiquitous expression. Our

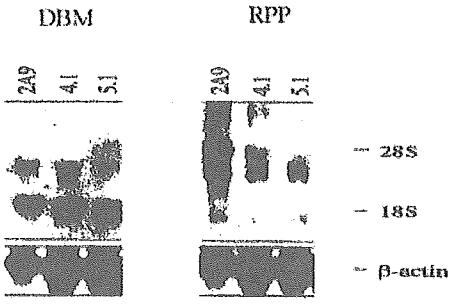

Fig. 4. Expression of DBM and RPP by thymic epithelial and stromal cell lines. RNA (20 μg) from various thymic epithelial and stromal cell lines were assayed by Northern blot with DBM- or RPP-specific probes.

data demonstrate that the RNA encoding the peptides RPP and DBM are expressed in thymic epithelial cell lines.

To further the candidacy of these two peptides as participants in the positive selection process *in vivo*, we examined whether the DBM and RPP peptides were presented by the MHC molecules from the thymic epithelial cell lines. The peptides presented by H-2D^b were purified from the thymic epithelial 2A9 cells. The isolated peptides were analyzed by reverse-phase HPLC fractionation and both DBM and RPP were detected in elution fractions (Fig. 5, and data not shown). To confirm that the peptides in these elution fractions included the DBM and RPP peptides, the elution fractions were analyzed by nanoflow HPLC microelectrospray ionization mass spectrometry. The fraction suspected to contain DBM was demonstrated to contain a peptide that yielded fragmentation ions corresponding to those expected from the DBM peptide, as shown in Fig. 5. Similarly, the fraction suspected of containing the RPP peptide also demonstrated the expected fragmentation ions (Fig. 5). These data, combined with the Northern-blot analysis, indicate that peptides DBM and RPP were expressed and presented by thymic epithelial cells. Therefore, two self-peptides that potentially mediate positive selection of virus-specific T cells were identified.

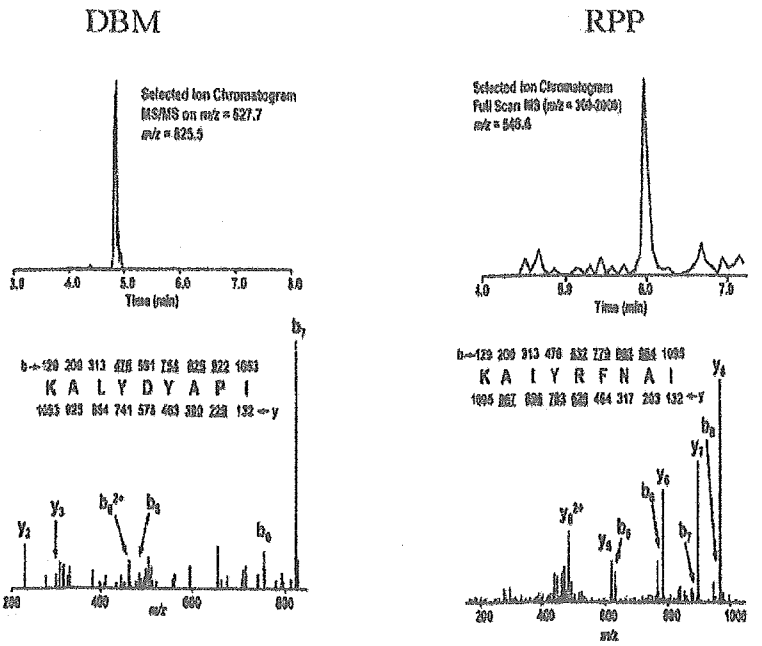

Fig. 5. Presentation of DBM and RPP peptide by thymic epithelial and stromal cell lines. Selected ion chromatogram for DBM in fraction 30 and for RPP in fraction 25 of the 2A9 cell line extract. The MS/MS spectrum for the *m/z*=527.7, the +2 charge state of DBM, and the *m/z*=548.6, the +2 charge state of RPP, are shown. Note that for RPP all of the abundant fragment ions correspond to the b-type (fragment ions containing the N terminus) and y-type (fragment ions containing the C terminus) sequence specific ions. Predicted type b- and y-fragment ions for DBM and RPP are shown above and below, respectively, the sequence. Ions observed in the mass spectrum are underlined.

2.5 Positively selecting peptides demonstrate different abilities to tune activation thresholds

Previous work in our laboratory has shown that T cells selected by a defined peptide lose their ability to respond to that peptide as mature cells [10–12]. The ability of the DBM and RPP peptides to tune the activation threshold of T cells expressing the P14 TCR was examined. Thymic lobes from $\beta2m^{-/-}$ P14 $TCR^{+/+}$ mice were incubated with DBM or RPP peptides at 10^{-4} M. The selected $CD8^+$ cells were purified and co-cultured with splenocytes that had been pulsed with various concentrations of different peptides.

Thymocytes selected by DBM were unable to proliferate to DBM-pulsed APC even at high concentrations (10^{-3} M) (Fig. 6A). These cells were functional, however, since vigorous proliferation was detected in response to the strong agonist ligand p33. These findings demonstrate that the DBM peptide was able to modulate the T cell activation threshold during thymic selection such that the mature T cells lose their ability to respond to signals mediated by this peptide.

Notably, RPP modified T cell responsiveness in a dose-dependent manner. When T cells were stimulated with 10^{-4} M of the RPP peptide, no proliferation was observed. This is consistent with the ability of positively selecting ligands to tune the mature T cell response. Yet, when these same cells were stimulated by APC pulsed with 10^{-3} M of RPP, proliferation was observed (Fig. 6A). This proliferation was reduced compared with the strong agonist p33 but nonetheless demonstrated that mature RPP-selected T cells were still able to respond to higher concentrations of RPP. The fact that thymocytes selected by either DBM or RPP were unable to proliferate in response to the selecting ligands demonstrates that the increase in $CD8^+$ cells in FTOC was due to positive selection events and not simply due to a proliferative

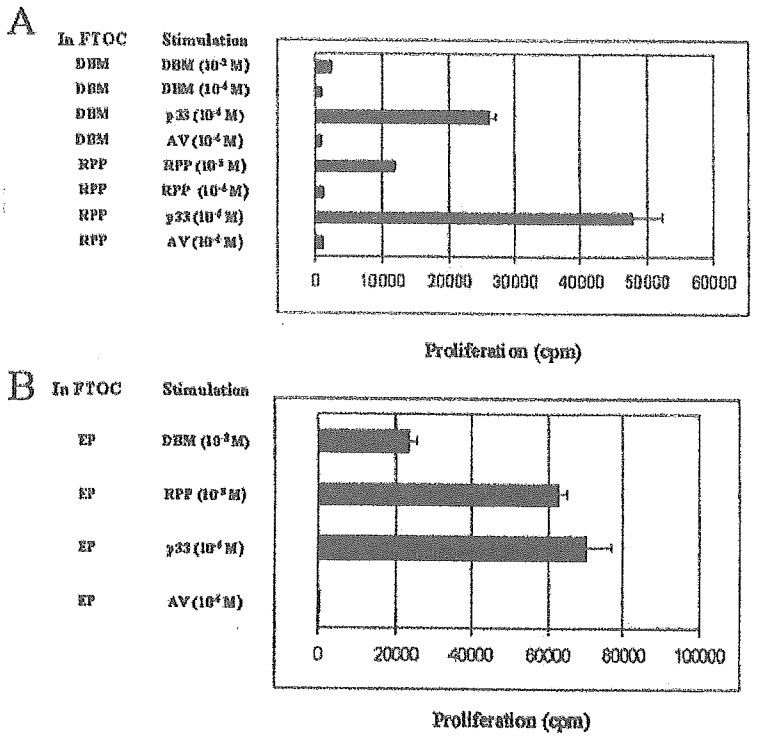

Fig. 6. Peptides DBM and RPP display different abilities to tune the T cell response. (A) SP $CD8^+$ Vα2 cells selected with either DBM or RPP at 10^{-4} M from day 16 fetal thymic lobes from TCR^+ $\beta2m^{-/-}$ mice were purified and then stimulated *in vitro* by irradiated total splenocytes from C57BL/6 mice pre-pulsed with the concentration of peptide listed, for 16 h. Proliferation was measured using $[^3H]$thymidine incorporation; cpm, counts per minute. (B) SP $CD8^+$ Vα2 cells selected by endogenous peptides (EP) from day 16 fetal thymic lobes from TCR^+ $\beta2m^{+/+}$ mice were purified and then stimulated as above. The p33 peptide was used as a positive control and the AV peptide as a negative control.

expansion of reactive TCR transgenic cells. In addition, these data demonstrate that T cells can modify their sensitivity and response to different selecting and activating ligands.

To ensure that the difference in the ability to tune observed between DBM and RPP peptides was not solely due to the inability of DBM to induce proliferation in our system, we performed FTOC that would select the transgenic TCR ($\beta 2m^{+/+}$ P14 $TCR^{+/+}$) by a mixture of endogenous peptides. The SP $CD8^+$ cells were then purified and co-cultured with APC pulsed with DBM or RPP at 10^{-3} M, or with positive (p33) or negative (AV) control peptides. When selected on endogenous peptides, mature P14 T cells were found to respond to either DBM or RPP at 10^{-3} M (Fig. 6B). A higher amount of proliferation was observed with RPP than DBM at this concentration but this is in keeping with the fact that RPP appears to be a slightly stronger agonist than DBM (Fig. 1 and reference [16]). These findings indicate that DBM and RPP peptides are able to differentially tune the activity of positively selected T cells.

3 Discussion

We have identified two weak agonist self-peptides that are able to mediate positive selection of a virus-specific TCR in FTOC. By employing HPLC and mass spectrometry we have demonstrated that MHC molecules expressed by thymic cell lines present these peptides. Moreover, we have shown that the two peptides display differential abilities to modulate the activation threshold of T cells selected in the presence of the peptides.

The self-peptides (DBM and RPP) bear little direct amino acid homology to the viral agonist peptide. DBM is homologous to p33 at only four out of nine amino acid residues whereas RPP shares only three common residues with p33 (See Fig. 1A). The shared residues are not those that are prevalent in the H-$2D^b$-associated peptide pool [29], nor are they predominantly the residues known to contact the TCR [12]. This implies that there are characteristics of peptides other than amino acid sequence that are important for TCR–peptide–MHC interactions. Findings of other groups support this assertion (see Table 1 for a summary of the results discussed below).

Hogquist et al. [2] and Santori et al. [6] found two self-peptides (CPα1 and Catnb) that positively selected T cells bearing the OT-1 transgenic TCR. These peptides demonstrated the conservation of charge at residues 6 and 7 with the known ligand OVAp. Ablation of this charge in these self-peptides severely hampered the ability to trigger the transgenic TCR but had no effect upon MHC binding.

Along with charge, the results of Hu et al. [3] and Sasada et al. [4] suggest that peptide conformation may also be important for interaction with the TCR. One of the self-

Table 1. Summary of natural peptides that are potential selecting ligands

TCR	Selecting peptide[a]				Specificity[a]		References
	Name	Sequence	Type	Ligand	Sequence	MHC	
OT-1	CPαI	I**S**F**K**F**D**H**L**	Antagonist	OVAp	S**I**I**N**F**E**K**L**	H-$2K^b$	[2, 6]
OT-1	Catnb	R**T**Y**T**Y**E**K**L**	Antagonist	OVAp	S**I**I**N**F**E**K**L**	H-$2K^b$	[6]
H-Y	$Ubelx_{509-517}$	**K**S**N**L**N**R**Q**F**L**	Antagonist	Smcy	K**C**S**R**N**R**Q**Y**L**	H-$2D^b$	[5]
P14	RR	F**Q**I**V**N**P**H**L**L**	Antagonist	p33	K**A**V**Y**N**F**A**T**M**	H-$2D^b$	[3]
F5	BP	N**S**I**R**N**L**D**T**I**	Antagonist	IF-68	A**S**N**E**N**M**D**A**M	H-$2D^b$	[3]
F5	HH	L**A**I**R**N**D**E**E**L**	Antagonist	IF-68	A**S**N**E**N**M**D**A**M	H-$2D^b$	[3]
PCC	PCC50V54A	**AEGFSYTVANKAKGIT**	Agonist	PCC50V	AEGFSYTVANKNKGIT	I-A^b	[33][b]
N15	$NubO_{68-75}$	V**N**V**D**Y**S**K**L**	Agonist	VSV8	R**G**Y**V**Y**Q**G**L**	H-$2K^b$	[4]
P14	DBM	**K**A**L**Y**D**Y**A**P**I**	Agonist/ antagonist	p33	K**A**V**Y**N**F**A**T**M**	H-$2D^b$	This paper
P14	RPP	**K**A**I**Y**R**F**N**A**I**	Agonist/ antagonist	p33	K**A**V**Y**N**F**A**T**M**	H-$2D^b$	This paper

[a] MHC anchor residues are underlined and amino acid residues shared between the known ligand of the TCR and the selecting peptide are bolded in the selecting peptide.
[b] This group has not formally demonstrated that PCC50V54A is naturally processed and presented by MHC molecules.

peptides identified by Hu et al. mediated positive selection of the P14 TCR. This peptide shared only one amino acid residue in common with the p33 peptide, a known MHC anchor residue. Similarly, Sasada et al. [4] identified a self-peptide capable of mediating positive selection of a virus-specific N15 TCR. The peptide was only homologous at two residues to the VSV8 peptide antigen and both of those residues are known anchor residues for binding MHC. Yet, the peptide identified by Sasada et al. [4] was clearly interacting with the N15 TCR because it displayed weak agonist properties. This result, combined with the results of Hu et al. [3] and our own, demonstrates that the ability to interact with a defined TCR does not depend upon direct sequence homology. Rather, it is likely that these peptides have conformational similarities when presented by defined MHC molecules.

Interestingly, the rat DBM peptide (KALYNYAPI) has been crystallized in the H-2D^b molecule (A. Achour, personal communication). The crystal structure is strikingly similar to the native LCMV-gp peptide (KAVYNFATC) that has been shown to mediate positive selection of functional cells at low concentrations [18, 19, 30]. All of these findings support the interpretation that the TCR requires interactions with a conserved element — be it sequence, charge or conformation — to promote positive selection.

The mouse peptides DBM and RPP are natural agonist ligands with antagonist activity [16]. A natural ligand defined for positive selection of the N15 VSV-virus-specific TCR was also an agonist ligand [4]. Extensive discussion continues to evolve around whether a selecting ligand is an agonist or antagonist [1, 31–33]. This, however, is a moot point for several reasons. Firstly, antagonist activity is measured on mature T cells and it is clear that the properties of mature T cells are significantly different than thymocytes. Mature T cells use PKCθ [34], Bcl-10 [35] and calcineurin [36], whereas studies fail to demonstrate a role for these molecules in DP thymocyte signaling. Immature thymocytes signal via c-Cbl [37, 38] whereas mature T cells do not. Furthermore, almost every agonist has antagonist properties depending upon the assay chosen, and many antagonists defined in the literature have agonist activity at high peptide concentrations [39–41].

In accordance with the findings of the other groups who identified self-peptides capable of positively selecting thymocytes [2–5], one of the self-peptides we identified was derived from a ubiquitously expressed gene. Collectively these data suggest that the self-peptides presented in the thymus that mediate positive selection of the T cell repertoire are also found and presented in the periphery. The precise mechanisms of tolerance that prevent these selected T cells from reacting against these self-peptides remain ill-defined. Evidence suggests that T cells require survival signals to be maintained in the periphery, and that these survival signals may be similar to positive selection signals in the thymus [42–44]. Our data suggest that interactions that promote survival signals in the thymus, and potentially similar to interactions in the periphery, alter lymphocyte activation thresholds such that they are unresponsive to the basal survival stimulation level. Recently, in support of this idea, Stefanova et al. [45] have elegantly demonstrated *in vivo* that contact with self-peptide–MHC complexes maintains T cell responsiveness to foreign peptides.

An understanding of the tuning mechanism may also provide insight into the initiation of autoimmunity. It would be interesting to determine whether autoimmune antigens are unable to tune T cells *in vivo* and therefore become targets that predispose individuals to autoimmunity. Further understanding of the nature of this flexibility may provide further insight into ways to manipulate T cell responsiveness to autoimmune or tumor-associated antigens.

4 Materials and methods

4.1 RMA-S stabilization assay

RMA-S cells were cultured overnight at 29°C in RPMI containing 10% FCS. Cells (0.5×10^6) were incubated with various concentrations of peptides for 3 h at 37°C. H2-D^b expression was analyzed by staining with monoclonal antibody B22.249 and FITC-conjugated rat anti-mouse Ig (Sigma). Data were calculated as follows: % mean above background = 100 × [{mean intensity of H-2D^b expression on RMA-S cells cultured with test peptide – mean intensity of H-2D^b expression on RMA-S cells cultured with the negative control peptide} / (mean intensity of H-2D^b expression on RMA-S cells cultured with the negative control peptide)].

4.2 Proliferation assays

Animals used in these studies were handled according to institutional guidelines. Spleen cells (2×10^6) from transgenic mice were co-cultivated with various concentrations of peptides for 2 days. Proliferation was monitored by the addition of 1 μCi [^{3}H]thymidine (Amersham). Cells were harvested and counted on a direct β-counter Matrix 96 (Canberra Packard Canada Ltd.). For the proliferation assays of SP CD8$^+$ cells selected in FTOC (see below), CD8$^+$ cells were first purified. Purification was done using magnetic microbead separation in a MACS column (Miltenyi Biotec, Ger-

many). Briefly, DP and SP CD4$^+$ cells were depleted using anti-CD4-microbeads. The negative fraction was then subjected to further purification of SP CD8$^+$ cells using anti-CD8-microbeads. The purified SP CD8$^+$ cells were then co-cultured with peptide-pulsed APC for 2 days. Cells were harvested and counted on a direct β-counter Matrix 96. The APC used were irradiated total splenocytes from C57BL/6 mice; the APC had been incubated *in vitro* for 48 h and the pulsed with the peptide for 16 h before the addition of the CD8$^+$ cells.

4.3 FTOC

Day 16 fetal thymic lobes were cultured in the presence of peptides and 2.5 μg/ml β2m (Sigma), 1X nutridoma (Boehringer Mannheim), IMDM and antibiotics. Peptides were added once or twice per day. After 6 days of culture, thymocytes were analyzed using the indicated antibodies (PharMingen) or were treated as described above for proliferation assays.

4.4 Northern blotting analysis

RNA was extracted by TRIZOL (Gibco) from various thymic epithelial or stromal cell lines: 2A9 [25], 4.1 (Hugo et al., unpublished) and 5.1 [26]. 20 μg of RNA was electrophoresed in a 1% agarose gel, transferred to Hybond N, and hybridized with probes from DBM cDNA [27] or PCR product from RPP [28] in 3X SCC, 1X Denhardts, and 100 μg/ml salmon sperm DNA at 65°C. PCR primers were AGAGAACTCCTAAACCTGATA and GCATTCTTCTACACGATAACA. After washing, the filter was analyzed on a phosphoimager after 5 days exposure. β-actin was included as a control.

4.5 H-2D^b isolation and peptide purification

H-2D^b-bound peptides were isolated according to the methods of Rammensee et al. [46] with several modifications. 2A9 cells were pelleted and lysed by vortexing at 0–4°C using 1×10^8 cells ml^{-1} in fresh complete lysis buffer [Tris 0.1 M pH 8.3, NaCl 0.05 M, $MgCl_2$ 1 mM, NaN_3 0.02%, phenylmethylsufonylfluoride 1 mM, iodoacetamide 10 mM and Surfact-Amps purified NP-40 (SA-NP-40, stored under nitrogen; Pierce, Rockford, IL) 0.5%]. Debris was pelleted, and the supernatant flash-frozen in liquid nitrogen and stored at –70°C. In preparation for class I purification, frozen aliquots were rapidly thawed at 4°C in a water bath and were pooled and cleared by ultracentrifugation (100,000×g, 30 min) followed by filtration (0.8 μ).

Affinity matrices were prepared by incubating B22-249.R1 (B22 anti-H2-D^b, 1 mg [47]) or H16-L10-4R5 (ATCC HB-65, anti-influenza nucleoprotein [48]) with TSK gel AF-protein A Toyopearl 650 M (Toso Corporation, Tokyo) in HPLC Tris buffer (0.1 M Tris pH 8.1, 0.05 M NaCl, 0.02% NaN_3). The matrices were packed into HPLC columns and washed individually to background absorbance (280 nm) using HPLC Tris with added SA-NP-40 (0.5%) and then plumbed in series, with the control antibody column first. Cleared cell lysate (2A9 cells, 22 ml) was run over the columns at 0.2–0.5 ml/min, followed by a wash to background absorbance with HPLC Tris with SA-NP-40 (15 ml) and then HPLC Tris (no SA-NP-40) to background absorbance and borate buffer (pH 8.1, about 25 ml, $Na_2B_2O_7$ 0.1 mM, NaCl 0.05 mM, NaN_3 0.02%). The columns were separated and plumbed individually in the reverse direction and eluted using freshly prepared 0.2 N aldehyde-free acetic acid (Caledon, Georgetown, ON). The prominent peak was collected in a single fraction of 2–3 ml. Aldehyde-free acetic acid was added to the eluate to a concentration of 10% and the solution was heated to 100°C for 7–10 min. The mixture was ultrafiltered overnight (Ultrafree-CL, 5000 NMWL, Millipore, Bedford, MT), and the low-molecular-weight material was evaporated to about 0.75 ml under vacuum. HPLC-grade water was added to 2 ml and the evaporation was repeated. Salts, acetic acid, and non-peptide impurities were removed by running each solution in multiple injections onto reverse-phase C18 HPLC columns, and washing to background absorbance with water plus 0.1% trifluoroacetic acid (TFA). The solvent flow in the C18 column was then reversed and the peptides were eluted in a single bolus using 50% acetonitrile plus 0.1% TFA.

4.6 Reverse-phase HPLC fractionation of the extracted peptides

Reverse-phase HPLC fractionation of the extracted MHC class I peptides was performed on an Applied Biosystems 130A HPLC (Foster City, CA) with a narrowbore (2.1 mm × 40 mm, 5 μM particles) Higgins HAISIL C18 column (Winter Park, FL). The elution gradient was 0–15% B (5 min), 15–60% B (6–55 min), 60–100% B (56–62 min). Solvent A was 0.1% TFA (HPLC grade, Applied Biosystems, Foster City, CA) in NANOpure water (Barnstead, Dubuque, IA), and solvent B was 0.085% TFA in 60% acetonitrile (HPLC grade, Mallickrodt, Paris, KY). One-minute fractions were collected manually at a flow rate of 200 μl/minute.

4.7 Mass spectrometric analysis of DBM

An aliquot containing approximately 4% (2 μl loaded out of 50 μl total volume) of the fraction containing DBM was analyzed by nanoflow HPLC microelectrospray ionization mass spectrometry [24]. A Finnigan LCQ ion trap mass spectrometer (Thermoquest, San Jose, CA) was set up to repeatedly dissociate (through collision-activated dissociation), the specific mass (m/z=527.7) corresponding to the +2 charge state of the KALYDYAPI peptide. The cell surface copy number of the DBM peptide was roughly quantitated using synthetic DBM peptide as a standard in a separate run.

4.8 Mass spectrometric detection of RPP

An aliquot containing approximately 2% (1 µl loaded out of 50 µl total volume) of the fraction containing RPP was analyzed by nanoflow HPLC microelectrospray ionization mass spectrometry [49]. The Finnigan LCQ ion trap mass spectrometer was operated in data-dependant mode, in which the five most abundant ions in a given MS scan were sequentially subjected to collision-activated dissociation. The cell surface copy number of the RPP peptide was roughly quantitated using synthetic RPP peptide as a standard in a separate run.

Acknowledgements: This work was supported by the Terry Fox Program Project from the National Cancer Institute of Canada (to P. S. O.), and U.S. Public Health Service Grant 2-R37-AI 33993 (to D. F. H.). We thank Shirley Ho for technical assistance.

References

1 **Sebzda, E., Mariathasan, S., Ohteki, T., Jones, R., Bachmann, M. F. and Ohashi, P. S.,** Selection of the T cell repertoire. *Annu. Rev. Immunol.* 1999. **17:** 829–874.

2 **Hogquist, K. A., Tomlinson, A. J., Kieper, W. C., McGargill, M. A., Hart, M. C., Naylor, S. and Jameson, S. C.,** Identification of a naturally occurring ligand for thymic positive selection. *Immunity* 1997. **6:** 389–399.

3 **Hu, Q., Bazemore Walker, C. R., Girao, C., Opferman, J. T., Sun, J., Shabanowitz, J., Hunt, D. F. and Ashton-Rickardt, P. G.,** Specific recognition of thymic self-peptides induces the positive selection of cytotoxic T lymphocytes. *Immunity* 1997. **7:** 221–231.

4 **Sasada, T., Ghendler, Y., Neveu, J. M., Lane, W. S. and Reinherz, E. L.,** A naturally processed mitochondrial self-peptide in complex with thymic MHC molecules functions as a selecting ligand for a viral-specific T cell receptor. *J. Exp. Med.* 2001. **194:** 883–892.

5 **Santori, F. R., Brown, S. E., Lu, Y., Neubert, T. A. and Vukmanovic, S.,** Cutting edge: Positive selection induced by a self-peptide with TCR antagonist activity. *J. Immunol.* 2001. **167:** 6092–6095.

6 **Santori, F. R., Kieper, W. C., Brown, S. M., Lu, Y., Neubert, T. A., Johnson, K. L., Naylor, S., Vukmanovic, S., Hogquist, K. A. and Jameson, S. C.,** Rare, structurally homologous self-peptides promote thymocyte positive selection. *Immunity* 2002. **17:** 131–142.

7 **Grossman, Z. and Paul, W. E.,** Adaptive cellular interactions in the immune system: the tunable activation threshold and the significance of subthreshold responses. *Proc. Natl. Acad. Sci. USA* 1992. **89:** 10365–10369.

8 **Grossman, Z. and Singer, A.,** Tuning of activation thresholds explains flexibility in the selection and development of T cells in the thymus. *Proc. Natl. Acad. Sci. USA* 1996. **93:** 14747–14752.

9 **Grossman, Z. and Paul, W. E.,** Autoreactivity, dynamic tuning and selectivity. *Curr. Opin. Immunol.* 2001. **13:** 687–698.

10 **Kawai, K. and Ohashi, P. S.,** Immunological function of a defined T cell population tolerized to low-affinity self antigens. *Nature* 1995. **374:** 68–69.

11 **Sebzda, E., Kündig, T. M., Thomson, C. T., Aoki, K., Mak, S. Y., Mayer, J., Zamborelli, T. M., Nathenson, S. and Ohashi, P. S.,** Mature T cell reactivity altered by a peptide agonist that induces positive selection. *J. Exp. Med.* 1996. **183:** 1093–1104.

12 **Mariathasan, S., Bachmann, M. F., Bouchard, D., Ohteki, T. and Ohashi, P. S.,** Degree of TCR internalization and Ca^{2+} flux correlates with thymocyte selection. *J. Immunol.* 1998. **161:** 6030–6037.

13 **Wong, P., Barton, G. M., Forbush, K. A. and Rudensky, A. Y.,** Dynamic tuning of T cell reactivity by self-peptide-major histocompatibility complex ligands. *J. Exp. Med.* 2001. **193:** 1179–1187.

14 **Williams, O., Tarazona, R., Kioussis, D., Harker, N. and Roderick, K.,** Interactions with multiple peptide ligands determine the fate of developing thymocytes. *Proc. Natl. Acad. Sci. USA* 1998. **95:** 5706–5711.

15 **Nicholson, L. B., Anderson, A. C. and Kuchroo, V. K.,** Tuning T cell activation threshold and effector function with cross-reactive peptide ligands. *Int. Immunol.* 1999. **12:** 205–213.

16 **Ohteki, T., Hessel, A., Bachmann, M. F., Zakarian, A., Sebzda, E., Teao, M. S., McKall-Faienza, K., Odermatt, B. and Ohashi, P. S.,** Identification of a cross-reactive self ligand in virus-mediated autoimmunity. *Eur. J. Immunol.* 1999. **29:** 2886–2896.

17 **Townsend, A., Oehlen, C., Bastin, J., Ljunggren, H.-G., Foster, L. and Kärre, K.,** Association of class I major histocompatibility heavy and light chains induced by viral peptides. *Nature* 1989. **340:** 443–448.

18 **Sebzda, E., Wallace, V. A., Mayer, J., Yeung, R. S. M., Mak, T. W. and Ohashi, P. S.,** Positive and negative thymocyte selection induced by different concentrations of a single peptide. *Science* 1994. **263:** 1615–1618.

19 **Ashton-Rickardt, P. G., Bandeira, A., Delaney, J. R., Van Kaer, L., Pircher, H. P., Zinkernagel, R. M. and Tonegawa, S.,** Evidence for a differential avidity model of T cell selection in the thymus. *Cell* 1994. **76:** 651–663.

20 **Hogquist, K. A., Jameson, S. C. and Bevan, M. J.,** Strong agonist ligands for the T cell receptor do not mediate positive selection of functional $CD8^+$ T cells. *Immunity* 1995. **3:** 79–86.

21 **Chidgey, A. and Boyd, R.,** Agonist peptide modulates T cell selection thresholds through qualitative and quantitative shifts in CD8 co-receptor expression. *Int. Immunol.* 1997. **9:** 1527–1536.

22 **Hogquist, K. A., Jameson, S. C., Heath, W. R., Howard, J. L., Bevan, M. J. and Carbone, F. R.,** T cell receptor antagonist peptides induce positive selection. *Cell* 1994. **76:** 17–27.

23 **McGargill, M. A., Derbinski, J. M. and Hogquist, K. A.,** Receptor editing in developing T cells. *Nat. Immunol.* 2000. **1:** 336–341.

24 **Takahama, Y., Shores, E. W. and Singer, A.,** Negative selection of precursor thymocytes before differentiation into $CD4^+CD8^+$ cells. *Science* 1992. **258:** 653–656.

25 **Hugo, P., Kappler, J. W. and Marrack, P. C.,** Positive selection of TCR$\alpha\beta$ thymocytes: Is cortical thymic epithelium an obligatory participant in the presentation of major histocompatibility complex protein? *Immunol. Rev.* 1993. **135:** 133–155.

26 **Hugo, P., Kappler, J. W., Godfrey, D. I. and Marrack, P. C.,** Thymic epithelial cell lines that mediate positive selection can also induce thymocyte clonal deletion. *J. Immunol.* 1994. **152:** 1022–1034.

27 **Nakano, T., Kobayashi, K., Saito, S., Fujita, K. and Nagatsu, T.,** Mouse dopamine β-hydroxylase: primary structure deduced from the cDNA sequence and exon/intron organization of the gene. *Biochem. Biophys. Res. Commun.* 1992. **189:** 590–599.

28 **Loeb, D. D., Padgett, R. W., Hardies, S. C., Shehee, W. R., Comer, M. B., Edgell, M. H. and Hutchison, C. A.,** The sequence of a large L1Md element reveals a tandemly repeated 5′ end and several features found in retrotransposons. *Mol. Cell. Biol.* 1986. **6:** 168–182.

29 **Dalloul, A. H., Ngo, K. and Fung-Leung, W. P.,** CD4-negative cytotoxic T cells with a T cell receptor α/β intermediate expression in CD8-deficient mice. *Eur. J. Immunol.* 1996. **26:** 213–218.

30 **Mariathasan, S., Ho, S. S. N., Zakarian, A. and Ohashi, P. S.,** Degree of ERK activation influences both positive and negative thymocyte selection. *Eur. J. Immunol.* 2000. **30:** 1060–1068.

31 **Viret, C., He, X. and Janeway, C. A. Jr.,** Paradoxical intrathymic positive selection in mice with only a covalently presented agonist peptide. *Proc. Natl. Acad. Sci. USA* 2001. **98:** 9243–9248.

32 **Chiu, N. M., Wang, B., Kerkaik, K. M., Kurlander, R., Pamer, E. G. and Wang, C.-R.,** The selection of M3-restricted T cells is dependent on M3 expression and presentation of *N*-formylated peptides in the thymus. *J. Exp. Med.* 1999. **190:** 1869–1878.

33 **Kraj, P., Pacholczyk, R., Ignatowicz, H., Kieielow, P., Jensen, P. and Ignatowicz, L.,** Positive selection of CD4$^+$ T cells is induced *in vivo* by agonist and inhibited by antagonist peptides. *J. Exp. Med.* 2001. **194:** 407–416.

34 **Sun, Z., Arendt, C. W., Ellmeier, W., Schaeffer, E. M., Sunshine, M. J., Gandhi, L., Annes, J., Petrzilka, D., Kupfer, A., Schwartzberg, P. L. and Littman, D. R.,** PKC-θ is required for TCR-induced NF-κB activation in mature but not immature T lymphocytes. *Nature* 2000. **404:** 402–407.

35 **Ruland, J., Duncan, G. S., Elia, A., Barrantes, I. d. B., Nguyen, L., Millar, D. G., Bouchard, D., Wakeham, A., Ohashi, P. S. and Mak, T. W.,** Bcl10 is a positive regulator of antigen receptor-induced activation of NF-κB and neural tube closure. *Cell* 2001. **104:** 33–42.

36 **Chan, V. S. F., Wong, C. and Ohashi, P. S.,** Calcineurin Aα plays an exclusive role in TCR signaling in mature but not in immature T cells. *Eur. J. Immunol.* 2002. **32:** 1223–1229.

37 **Murphy, M. A., Schnall, R. G., Venter, D. J., Barnett, L., Bertoncello, I., Thien, C. B. F., Langdon, W. Y. and Bowtell, D. D. L.,** Tissue hyperplasia and enhanced T cell signalling via ZAP-70 in c-Cbl-deficient mice. *Mol. Cell. Biol.* 1998. **18:** 4872–4882.

38 **Naramura, M., Kole, H. K., Hu, R.-J. and Gu, H.,** Altered thymic positive selection and intracellular signals in Cbl-deficient mice. *Proc. Natl. Acad. Sci. USA* 1998. **95:** 15447–15552.

39 **Bachmann, M. F., Speiser, D. E., Zakarian, A. and Ohashi, P. S.,** Inhibition of TCR-triggering by a spectrum of altered peptide ligands suggests the mechanism for TCR-antagonism. *Eur. J. Immunol.* 1998. **28:** 3110–3119.

40 **Bachmann, M. F. and Ohashi, P. S.,** The role of T cell receptor dimerization in T cell activation. *Immunol. Today* 1999. **20:** 568–576.

41 **Werlen, G., Hausmann, B. and Palmer, E.,** A motif in the αβ T cell receptor controls positive selection by modulating ERK activity. *Nature* 2000. **406:** 422–426.

42 **Takeda, S., Rodewald, H.-R., Arakawa, H., Bluethmann, H. and Shimizu, T.,** MHC class II molecules are not required for survival of newly generated CD4$^+$ T cells, but affect their long-term life span. *Immunity* 1996. **5:** 217–228.

43 **Ernst, B., Lee, D.-S., Chang, J. M., Sprent, J. and Surh, C. D.,** The peptide ligands mediating positive selection in the thymus control T cell survival and homeostatic proliferation in the periphery. *Immunity* 1999. **11:** 173–181.

44 **Surh, C. D. and Sprent, J.,** Homeostatic T cell proliferation: how far can T cells be activated to self-ligands? *J. Exp. Med.* 2000. **192:** F9–F14.

45 **Stefanova, I., Dorfman, J. R. and Germain, R.,** Self-recognition promotes the foreign antigen sensitivity of naive T lymphocytes. *Nature* 2002. **420:** 429–434.

46 **Rammensee, H.-G., Falk, K. and Roetzschke, O.,** Peptides naturally presented by MHC class I molecules. *Annu. Rev. Immunol.* 1993. **11:** 213–244.

47 **Hammerling, G. J., Rusch, E., Tada, N., Kimura, S. and Hammerling, U.,** Localization of allodeterminants on H-2Kb antigens determined with monoclonal antibodies and H-2 mutant mice. *Proc. Natl. Acad. Sci. USA* 1982. **79:** 4737–4741.

48 **Yewdell, J. W., Frank, E. and Gerhard, W.,** Expression of influenza A virus internal antigens on the surface of infected infected P815 cells. *J. Immunol.* 1981. **126:** 1814–1819.

49 **Shabanowitz, J., Settlage, R. E., Marto, J. A., Christian, R. E., White, F. M., Russo, P. S., Martin, S. E. and Hunt, D. F.,** Sequencing the primordial soup. In *Proceedings of the 4th International Symposium on Mass Spectrometry in the Life and Health Sciences,* San Francisco, CA, August 25–29, 1998, pp 163–177.

Correspondence: Pamela S. Ohashi, University Health Network, Ontario Cancer Institute, 610 University Avenue, Toronto, Ontario M5G 2M9, Canada
Fax: +1–416–946–2086
e-mail: pohashi@uhnres.utoronto.ca

SAPK/JNK Signaling Participates in Embryonic Hepatoblast Proliferation via a Pathway Different from NF-κB-Induced Anti-Apoptosis

Hiroshi Nishina, Tomomi Watanabe, Kentaro Nakagawa, Shinya Ohata, Satoshi Asaka, and Toshiaki Katada

Summary. Mice lacking the stress-signaling kinases SEK1 and MKK7 die from embryonic day 10.5 (E10.5) to E12.5 with a defect in liver formation. However, the mechanism of the liver defect has remained unknown. In this review, we first introduce a monoclonal antibody, anti-Liv2, which specifically recognizes murine hepatoblasts, for the analysis of liver development, and further, we describe the genetic interaction of *sek1* with the tumor necrosis factor-α receptor 1 gene (*tnfr1*) and the protooncogene *c-jun*, which are also responsible for liver formation and cell apoptosis. The defective liver formation in $sek1^{-/-}$ embryos was not protected by an additional *tnfr1* mutation that rescues the embryonic lethality of mice lacking nuclear factor-kappa B (NF-κB) signaling components. There was a progressive increase in hepatoblast cell numbers in wild-type embryos from E10.5 to E12.5. In contrast, impaired hepatoblast proliferation was observed in $sek1^{-/-}$ livers from E10.5, although fetal liver-specific gene expression was normal. The impaired phenotype in $sek1^{-/-}$ livers was more severe than that in $c\text{-}jun^{-/-}$ embryos, and $sek1^{-/-}$ $c\text{-}jun^{-/-}$ embryos died earlier before E8.5. The hepatoblast proliferation required no hematopoiesis, because liver development was not impaired in $AML1^{-/-}$ mice, which lack hematopoietic functions. Stimulation of stress-activated protein kinase/c-Jun N-terminal kinase (SAPK/JNK) by hepatocyte growth factor was attenuated in $sek1^{-/-}$ livers. Thus, SEK1 and MKK7-mediated SAPK/JNK signaling appears to play a crucial role in hepatoblast proliferation and survival in a manner that is apparently different from that of NF-κB or c-Jun.

Key words. SEK1, NF-κB, SAPK/JNK, Hepatoblast, Hepatogenesis

Introduction

Embryonic liver formation consists of multiple stages and is under the influence of hormonal factors, as well as intercellular and matrix-cellular interactions. In mice, the initial event of liver ontogeny occurs around embryonic day 9 (E9), when epithelial cells of the foregut endoderm commit to become the liver primordium through their interaction with the cardiogenic mesoderm. The liver primordium proliferates and

Department of Physiological Chemistry, Graduate School of Pharmaceutical Sciences, The University of Tokyo, 7-3-1 Hongo, Bunkyo-ku, Tokyo 113-0033, Japan

invades the mesenchyme of the septum transversum to give rise to the hepatic codes and bud at E9.5. A critical genetic checkpoint in embryogenesis is the switch from yolk sac- and aorta-gonad-mesonephros region-dependent blood formation to liver-dependent hematopoiesis. This switch in the hematopoietic organ occurs from E10.5 to E12.5. The next major stage occurs around E14.5 when both hepatocytes and bile-duct epithelial cells arise embryologically from a common founder cell, the hepatoblast, which has bipotential differentiation capabilities in liver development [1,2].

The degree of hepatic maturation has been characterized by the expression of liver- and stage-specific genes [3,4]. Alphafetoprotein (AFP) is an early fetal hepatic marker (E9), and its expression decreases as the liver develops [5]. In contrast, the expression of albumin, the most abundant protein synthesized by hepatocytes, starts in early fetal hepatocytes (E12) and reaches the maximal level in the adult [6]. However, antibodies specific for AFP or albumin are not adequate to estimate the precise numbers of hepatoblasts in early fetal livers at E9.5–12.5, because both are diffusible serum proteins. Therefore, novel antibodies that clearly and specifically recognize individual hepatoblasts are required for studying fetal liver development in detail [7].

Recently, it has been shown by using ventral foregut endoderm isolated from mouse embryos at E8.25, that the close proximity of the cardiac mesoderm, which expresses fibroblast growth factors (FGFs) 1, 2, and 8, causes the foregut endoderm to develop into the liver [8,9]. On the other hand, another recent report has indicated a paracrine mechanism of late hepatogenesis that is derived from E14.5 murine embryos in cultured fetal liver cells. Blood cells in the fetal liver produce an interleukin (IL) 6-family cytokine, oncostatin M (OSM), to promote the development of hepatocytes [10]. However, the relationship between hepatogenesis and hematopoiesis in early fetal liver development remains unclear.

The stress-activated protein kinase/extracellular signal-regulated kinase kinases, SEK1/MKK4 and SEK2/MKK7, are direct activators of the stress-activated protein kinase (SAPK; also called c-Jun N-terminal kinase; JNK). Both are activated in response to a variety of cellular stresses, such as changes in osmolarity, metabolic poisons, DNA damage, heat shock, or the inflammatory cytokines, IL-1 and tumor necrosis factor-α (TNF-α). SEK1 and/or MKK7-mediated activation of SAPK/JNK phosphorylates c-Jun and activates c-Jun/Fos heterodimeric (AP-1) transcriptional complexes [11,12]. Several groups, including ours, have disrupted the *sek1* gene in mice, using homologous recombination [13–17]. SEK1-deficient embryos displayed severe anemia and died between E10.5 and E12.5. Hematopoiesis from yolk-sac precursors and vasculogenesis were normal in SEK1-deficient embryos. However, hepatogenesis and liver formation were severely impaired in the mutant embryos, and SEK1-deficient embryos had greatly reduced numbers of hepatocytes at E11.5–12.5. Although formation of the primordial liver and hepatic bud appeared to be normal, SEK1-deficient hepatocytes underwent massive apoptosis at E12.5 [15,17]. Embryos lacking the *c-jun* gene also display defective liver organization and die between E11.5 and E15.5 [18,19]. These results indicate that SEK1 and c-Jun provide a crucial and specific survival signal for fetal hepatogenesis. It is as yet unclear where SEK1 plays a role in hematopoietic cells or in hepatogenesis, what receptors trigger SEK1 activation, and what molecules regulate the SEK1-mediated signaling pathway in fetal liver development.

TNF-α elicits a wide range of biological responses, such as inflammation, tumor necrosis, differentiation, cell proliferation, and apoptosis, through the stimulation of

its receptor, TNFR1. Recently, it has been revealed that three separate signaling pathways, the induction of apoptosis, nuclear factor-kappa B (NF-κB) activation, and SEK1 and/or MKK7-mediated SAPK/JNK activation, are simultaneously mediated through TNFR1, and that SAPK/JNK activation appears to be not involved in the TNFR1-dependent induction of apoptosis, while the activation of NF-κB protects against the apoptosis [20]. Knockout mice for genes that are involved in NF-κB signaling have massive liver degeneration and apoptosis during midgestation, at E12.5–16. Such mice include knockout mice, for the RelA subunit of transcription factor NF-κB (died at E15–16), IκB kinase (β/IKK2; died at E12.5–14), NEMO/IKKγ (died at E12.5–13.0), and TRAF2-associated kinase T2K; died at E12.5–14.5) [21–26]. Importantly, the embryonic lethality and liver apoptosis observed in RelA-, IKK2- and T2K-knockout mice can be rescued by the simultaneous inactivation of TNFR1, suggesting that the apoptosis is induced by TNF-α circulating in the embryos [22,26,27]. However, the physiological role of the SEK1 and/or MKK7-mediated activation of SAPK/JNK in response to TNFR1 ligation remains to be resolved [20].

To understand the mechanisms of defective liver formation, we prepared monoclonal antibodies that specifically recognized murine fetal livers and characterized them using paraffin sections of embryos at various stages. One of the antibodies called anti-Liv2, specifically recognized so-called hepatoblasts at E9.5–12.5. We examined the relationship between the lethality of *sek1*$^{-/-}$ embryos and TNFR1-mediated apoptosis in mice lacking these genes. We found that *sek1*$^{-/-}$ *tnfr1*$^{-/-}$ double-mutant embryos delayed the beginning of liver resorption by 2 days compared with *sek1*$^{-/-}$ *tnfr1*$^{+/-}$ embryos, and that the liver defect was not rescued by the *sek1*$^{-/-}$ *tnfr1*$^{-/-}$ genotype. In addition, we investigated the ability of hepatoblast growth, as judged by the incorporation of bromodeoxyuridine (BrdU), in *sek1*$^{-/-}$ embryos at E10.5 before the occurrence of defective liver formation and massive apoptosis. We found a growth defect of hepatoblasts in *sek1*$^{-/-}$ embryos at E10.5. Furthermore, we showed that hepatoblasts could develop without hematopoiesis in early fetal liver at E9.5–11.5, using *AML1*$^{-/-}$ embryos, which lack definitive hematopoiesis [28,29]. The activation of SAPK/JNK by hepatocyte growth factor (HGF), observable in wild-type fetal livers, was markedly impaired in *sek1*$^{-/-}$ fetal livers. Thus, the lethality of *sek1* mutant embryos is most likely due to a defect that reflects SEK1 function and is not associated with NF-κB-induced anti-apoptosis in the cell growth of hepatoblasts [7].

A Novel Monoclonal Antibody, Anti-Liv2, Specifically Recognizes Hepatoblasts in Murine Embryos

To investigate fetal liver development in murine embryos at the early stage of E9.5–12.5, we prepared novel rat monoclonal antibodies against the fetal livers at E11.5 [7]. As shown in Fig. 1, one of the antibodies, anti-Liv2, specifically recognized hepatic cells that were co-stained with anti-HNF-3β antibody (Fig. 1A,B,D), but did not recognize TER119-positive erythrocytes. Although the nature of the Liv2 antigen has not been identified yet, the cell membrane of hepatic cells was stained with the monoclonal antibody, but the cytoplasm and nuclei were not (Fig. 1C). Almost all cells in the hepatic bud at E9.5 were recognized by anti-Liv2 (Fig. 1E,F). Interestingly, there was a progressive decrease in the ratio of Liv2-positive cells to the total number of

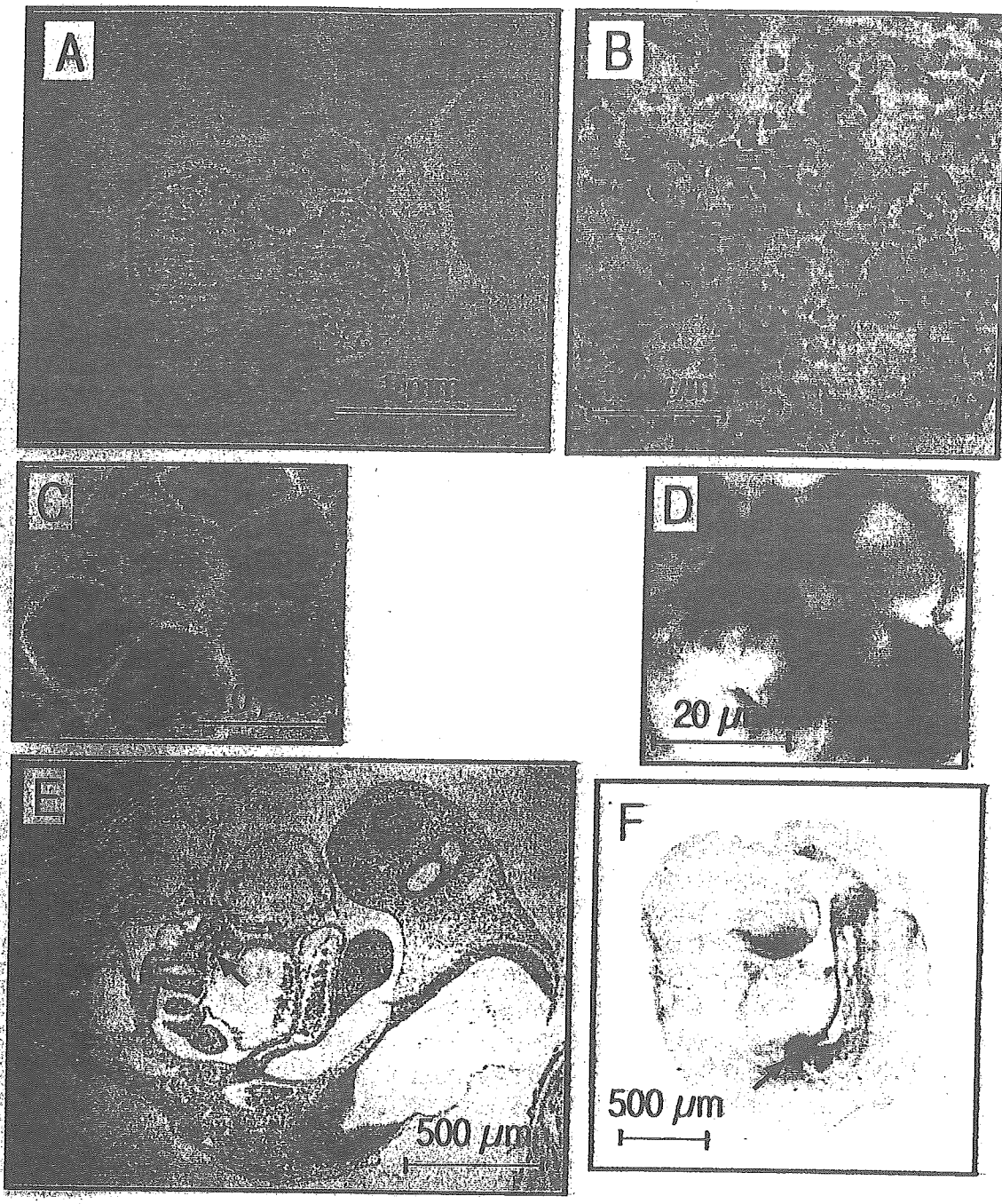

Fig. 1A–F. Characterization of a novel rat monoclonal antibody, anti-Liv2, which shows specific recognition of hepatoblasts in murine embryos. Transverse paraffin sections of murine embryonic livers at embryonic day 11.5 (E11.5) (A–C) and E9.5 (E), together with a frozen section at E11.5 (D) and a whole embryo at E9.5 (F), were stained with the rat monoclonal antibody, anti-Liv2. Positive cells exhibit a *brown* (A–C, and E) or *dark blue* (D and E) precipitate. D The frozen section containing Liv2-positive cells (*dark blue*) was further stained with anti-HNF-3β (*brown*). The *arrows* show hepatic buds

cells as the fetal liver developed from E9.5 to E12.5. Thus, it is very likely that anti-Liv2 specifically recognizes the so-called hepatoblasts that appear with fetal liver development. This monoclonal antibody was employed in the present study as a useful tool to analyze hepatoblasts in various mutant mice.

A Different Role of SEK1 from that of NF-κB-Induced Anti-Apoptosis in Fetal Liver Formation

As mentioned in the "Introduction", mice lacking SEK1 or NF-κB signaling components show embryonic lethality, with impaired liver formation, furthermore, the activation of both SEK1 and NF-κB is induced by TNFR1 in the fetal livers. Interestingly, liver apoptosis originating from the lack of NF-κB signaling components was rescued by the inactivation of TNFR1 [22,26,27]. Therefore, we investigated the relationship between SEK1- and TNFR1-mediated signaling pathways in whole embryos and fetal livers. C57BL/6-background *sek1*$^{-/-}$ *tnfr1*$^{-/-}$ embryos were prepared from *sek1*$^{+/-}$ *tnfr1*$^{-/-}$ intercrosses, and *sek1*$^{-/-}$ *tnfr1*$^{+/-}$ embryos were prepared from *sek1*$^{+/-}$ *tnfr1*$^{-/-}$ and *sek1*$^{+/-}$ *tnfr1*$^{+/+}$ intercrosses (Table 1). Embryos of all three expected genotypes from *sek1*$^{+/-}$ *tnfr1*$^{-/-}$ and *sek1*$^{+/-}$ *tnfr1*$^{+/+}$ intercrosses were not present at normal Mendelian ratios at E12.5 (Table 1, left side). Interestingly, embryos of all three expected genotypes from *sek1*$^{+/-}$ *tnfr1*$^{-/-}$ intercrosses were present at the normal Mendelian ratios until E13.5 and became abnormal at E14.5 (Table 1, right side). Embryo resorption was thus rescued by 2 days. The apparent sizes of *sek1*$^{-/-}$ *tnfr1*$^{-/-}$ embryos and livers were almost the same as those of the wild-type at E11.5 (Fig. 2A,B). However, liver defects were not rescued in *sek1*$^{-/-}$ *tnfr1*$^{-/-}$ embryos (Fig. 2E,G). The SEK1-deficient livers contained a capsule, hematopoietic precursors, and disorganized islands of Liv2-positive hepatoblasts (Fig. 2F), and these defects were still observed in *sek1*$^{-/-}$ *tnfr1*$^{-/-}$ livers (Fig. 2E,G). These results clearly indicate that embryo resorption is partially due to TNFR1-mediated signaling and that the role of SEK1 in fetal liver formation is different from that of NF-κB signaling, whose defects were rescued by inactivation of TNFR1 function.

Table 1. Analysis of embryos obtained from *sek1*$^{+/-}$ *tnfr1*$^{-/-}$ intercrosses or *sek1*$^{+/-}$ *tnfr1*$^{-/-}$ and *sek1*$^{+/-}$ *tnfr1*$^{+/+}$ intercrosses

Embryonic stage	*sek1*$^{+/+}$ *tnfr1*$^{+/-}$	*sek1*$^{+/-}$ *tnfr1*$^{+/-}$	*sek1*$^{-/-}$ *tnfr1*$^{+/-}$	*sek1*$^{+/+}$ *tnfr1*$^{-/-}$	*sek1*$^{+/-}$ *tnfr1*$^{-/-}$	*sek1*$^{-/-}$ *tnfr1*$^{-/-}$
E12.5	4	6	1*	12	34	15
E13.5	11	23	6*	17	33	17
E14.5	ND	ND	ND	9	16	1*

Asterisks indicate that embryos were under conditions of resorption

Embryos were isolated at the indicated time points of gestation and analyzed for Mendelian ratios of all three expected genotypes. Genotypes of embryos were determined by polymerase chain reaction (PCR), and the numbers of each genotype are listed in the Table.

ND, not determined

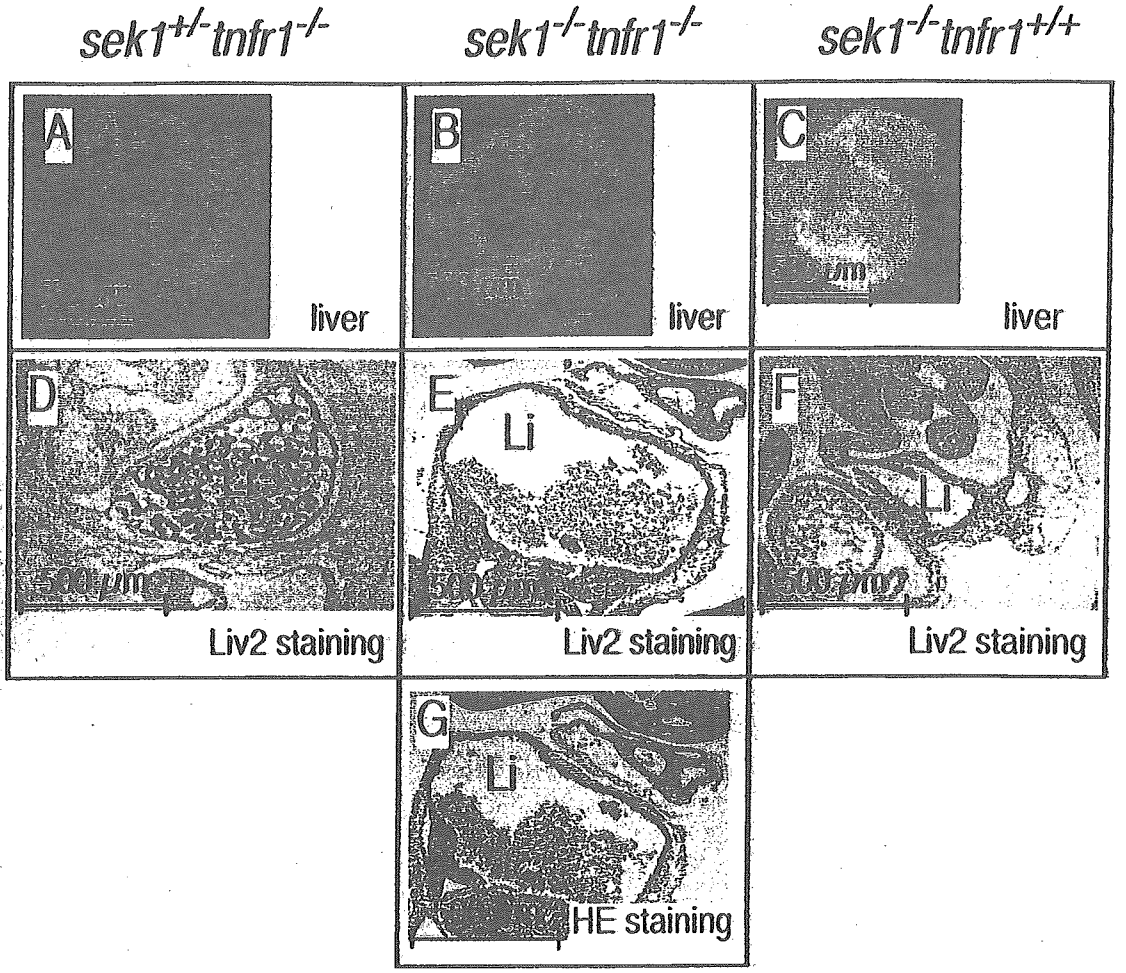

Fig. 2A–G. No rescue by tumor necrosis factory-α receptor 1 (TNFR1) inactivation of defective liver formation in *sek1*$^{-/-}$ embryos. Microscopic analysis was performed in *sek*$^{+/-}$ *tnfr1*$^{-/-}$ (A and D), *sek1*$^{-/-}$ *tnfr1*$^{-/-}$ (B, E, and G), and *sek1*$^{-/-}$ *tnfr1*$^{+/+}$ (C and F) fetal livers at E11.5. Transverse sections were stained with anti-Liv2 (D–F) and HE (G). *Li*, liver. *Bars*, 500 μm

SEK1-Deficient Livers Show a Decreased Number of Hepatoblasts in Early Hepatogenesis

To characterize *sek1*$^{-/-}$ livers, we determined numbers of Liv2-positive cells in *c-jun*$^{-/-}$ embryos, which also have defective liver formation [18,30]. Total cell numbers in *sek1*$^{-/-}$ and *c-jun*$^{-/-}$ livers were significantly lower than those in the wild-type liver. However, the ratio of Liv2-positive to the total number of liver cells was not significantly different among the three types of mice, and the ratios gradually decreased with liver development, being approximately 100% at E9.5, 60% at E10.5, 50% at E11.5, and 20% at E12.5. The number of Liv2-positive cells increased progressively, from 5×10^4 to 3×10^5 cells, during E10.5–12.5 in wild-type fetal livers. Although the numbers of Liv2-positive cells at E10.5 were not different among wild-type, *sek1*$^{-/-}$, and *c-jun*$^{-/-}$ livers, the progressive increase observed in wild-type livers was markedly attenuated

at E11.5 and E12.5 in *sek1*$^{-/-}$ and *c-jun*$^{-/-}$ livers, respectively. These results clearly indicate that impaired hepatoblast development certainly occurs in *sek1*$^{-/-}$ embryos and that *sek1* mutation is more severe than *c-jun* mutation in terms of hepatoblast development, which is consistent with the previous finding that *sek1*$^{-/-}$ embryos die earlier than *c-jun*$^{-/-}$ embryos.

SEK1-Deficient Livers Exhibit Normal Hepatic Gene Expression

A recent study has shown that *c-jun*$^{-/-}$ livers display the normal expression of the mRNAs, for albumin, keratin 18, hepatocyte HNF-1, β-globin, and erythropoietin, some of which are putative AP-1 target genes [30]. To confirm normal liver differentiation in *sek1*$^{-/-}$ embryos, the tissue-specific gene expression was measured by means of reverse transcription-polymerase chain reaction (RT-PCR). An early fetal hepatic marker, AFP, was expressed at the same level in wild-type and *sek1*$^{-/-}$ livers at E10.5 when cell numbers of Liv2-positive hepatoblasts were the same. Furthermore, a mature hepatic marker, albumin, was also expressed in both wild-type and *sek1*$^{-/-}$ fetal livers at E10.5 and E11.5. These results indicate that hepatic differentiation is not affected in *sek1*$^{-/-}$ fetal livers, similar to findings in *c-jun*$^{-/-}$ livers.

SEK1-Deficient Livers are Characterized as Showing Impaired Cell Growth of Hepatoblasts

We previously reported massive cell apoptosis in *sek1*$^{-/-}$ livers at E12.5 [15]. This apoptosis appeared to be associated with a decreased number of hepatoblasts at E11.5, without significant change in the gene expression of hepatic markers. Therefore, the growth capacity of *sek1*$^{-/-}$ hepatoblasts at the early stage of E10.5 was analyzed by the incorporation of bromodeoxyuridine (BrdU; Fig. 3). Interestingly, BrdU incorporation into Liv2-positive hepatoblasts was greatly reduced in *sek1*$^{-/-}$ livers compared with wild-type and *c-jun*$^{-/-}$ livers. These results suggest that *sek1* mutation may result in the impaired growth capacity of hepatoblasts at E10.5 when no other obvious defects in *sek1*$^{-/-}$ livers are observed.

Genetic Interaction Between *sek1* and *c-jun* in Murine Development

Because *sek1* and *c-jun* knockout mice display a similar phenotype of impaired liver formation [15], we further examined the genetic interaction between the two genes by preparing *sek1*$^{-/-}$ *c-jun*$^{-/-}$ double-mutant embryos. According to the Mendelian ratio (1 : 16), there was the expected number of the *sek1*$^{-/-}$ *c-jun*$^{-/-}$ genotype in E8.5 embryos, in addition to *sek1*$^{+/+}$ *c-jun*$^{+/+}$, *sek1*$^{-/-}$ *c-jun*$^{+/+}$, and *sek1*$^{+/+}$ *c-jun*$^{-/-}$ genotypes. No *sek1*$^{-/-}$ *c-jun*$^{-/-}$ embryos were, however, observed at E10.5, though embryos of the *sek1* or *c-jun* single mutant existed at the expected numbers. The loss of *sek1*$^{-/-}$ *c-jun*$^{-/-}$ embryos at E10.5 appeared to be due to resorption, because all the embryos at E8.5 were already dead. Thus, *sek1*$^{-/-}$ *c-jun*$^{-/-}$ double-mutant embryos died before E8.5 and underwent resorption through E10.5. These results indicate that the *sek1* and *c-jun* genes work synergistically during early embryonic development.

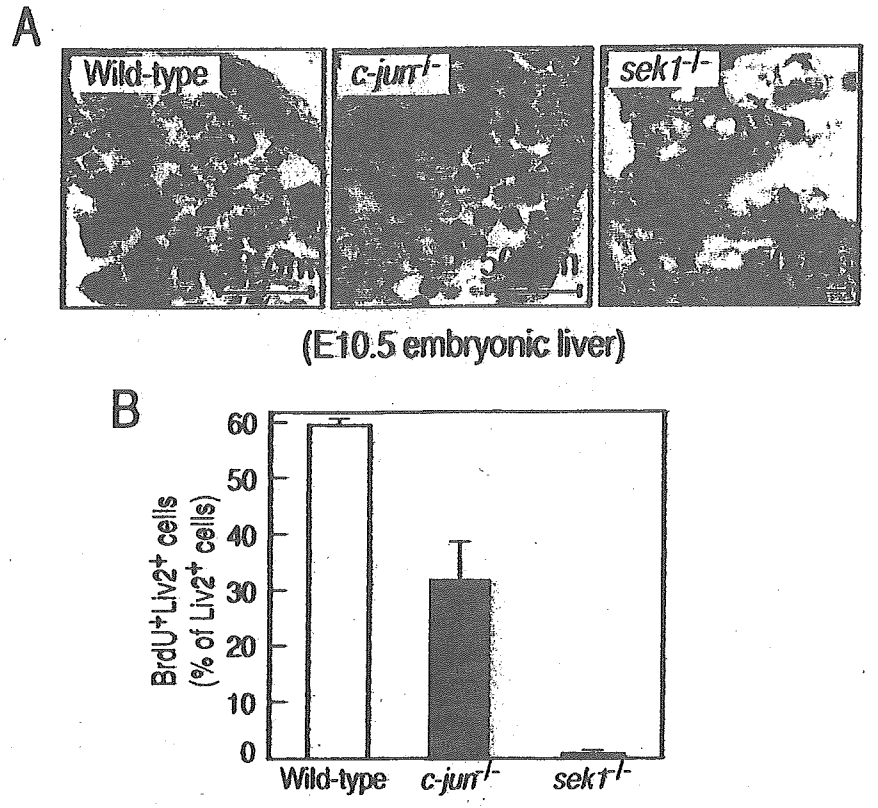

Fig. 3A,B. Impaired hepatoblast growth observed in *sek1*$^{-/-}$ livers. Pregnant mice bearing E10.5 embryos were injected with 0.3 ml of 50 mg/ml bromo-deoxyuridine (*BrdU*). After 4 h, the embryos were isolated, fixed with 4% paraformaldehyde, and genotypes of the embryos were determined by polymerase chain reaction (PCR). A Transverse sections were prepared from the paraffin embedding of wild-type (*left*), *c-jun*$^{-/-}$ (*middle*), and *sek1*$^{-/-}$ (*right*) embryos and stained with anti-Liv2 (*brown*). *Arrows* indicate BrdU-incorporated (*blue colored*) Liv2-positive hepatoblasts. B The BrdU-incorporated cells were counted in the three embryos (wild-type, *c-jun*$^{-/-}$, and *sek1*$^{-/-}$), and the values are expressed as percentages of the total of Liv2-positive hepatoblasts

No Requirement of Hematopoiesis for Hepatoblast Growth in Early Hepatogenesis

To examine the relationship between hepatoblast growth and hematopoiesis in early fetal liver, we measured the number of Liv2-positive cells at E11.5 in *AML1*$^{-/-}$ embryos, which lack definitive hematopoiesis. The total numbers of hepatic cells *plus* blood cells in wild-type and *AML1*$^{-/-}$ livers at E11.5 were counted, at 3.0×10^5 and 2.2×10^5 cells, respectively. When paraffin sections were prepared from E11.5 fetal livers and stained with anti-Liv2 or anti-TER119, there were 44% and 79% of Liv2-positive cells in wild-type and *AML1*$^{-/-}$ livers, respectively. *AML1*$^{-/-}$ fetal livers at E11.5 contained approximately 80% of Liv2-positive cells and 20% of TER119-positive primitive erythrocytes. Therefore, the numbers of Liv2-positive cells were calculated to be 1.3×10^5 and 1.7×10^5 in wild-type and *AML1*$^{-/-}$ livers, respectively. Thus, the cell numbers of hepato-

blasts were higher in *AML1*$^{-/-}$ livers than in wild-type onès. These results indicate that hematopoiesis and growth factors from blood cells are not essentially required for hepatoblast growth in early hepatogenesis.

Impairment of HGF-Induced SAPK/JNK Activation in Fetal Livers Lacking SEK1

To elucidate the biochemical interaction between SEK1 and SAPK/JNK, we first investigated whether HGF, which is produced by nonblood cells, could activate SAPK/JNK in fetal liver cells expressing the HGF receptor, c-Met. In a previous report [15], we could not detect any SAPK/JNK activation by HGF in a primary cell culture prepared from fetal livers. Therefore, in this study, we screened liver cells in an intact condition and found that strong SAPK/JNK activation was observed in response to HGF by using whole livers at E10.5, where about 60% of cells are Liv2-positive hepatoblasts. There was maximally a more than 25-fold increase in SAPK/JNK activity at 10 min, and the activity decreased rapidly. Such marked activation of SAPK/JNK was, however, greatly reduced in *sek1*$^{-/-}$ fetal livers. Interestingly, another member of the stress-activated mitogen activated protein (MAP) kinase family, p38, was constitutively phosphorylated without stimulation by HGF in fetal livers, and this phosphorylation was still observed in *sek1*$^{-/-}$ fetal livers. These results indicate that SEK1 is required for HGF-induced full activation of SAPK/JNK but not for p38 activation, and that HGF is one of the growth factors that regulate hepatoblast growth in early fetal liver development.

Conclusion

Embryonic liver formation is, genetically, a crucial checkpoint in fetal hematopoiesis and development. Although hematopoiesis has been characterized at the cellular and molecular levels, hepatogenesis and liver formation are just beginning to be characterized. To analyze early liver development, we first screened monoclonal antibodies that specifically recognized murine fetal livers by using transverse sections of E11.5 embryos. One of the antibodies, anti-Liv2, is applicable to paraffin sections and whole mount embryos, and the Liv2 antigen appears to be localized in the cell membrane (Fig. 1). The ratios of Liv2-positive cells from E9.5 to E12.5 were consistent with those of hepatic cells defined as hepatoblasts. Using anti-Liv2, we measured the exact cell numbers of hepatoblasts in fetal liver development in wild-type, *sek1*$^{-/-}$, and *c-jun*$^{-/-}$ mice. Thus, our experiments proved anti-Liv2 to be a useful tool for identifying murine hepatoblasts in early fetal livers, though the Liv2 antigen and its physiological role have not been determined yet.

Previously, we and another group reported that *sek1*$^{-/-}$ embryos died between E10.5 and E12.5, with a decreased number of cytokeratin-positive hepatocytes at E11.5, and massive hepatocyte apoptosis at E12.5 [15,17]. To extend the above results, we examined an interesting question: whether the hepatic apoptosis and embryonic lethality observed in *sek1*$^{-/-}$ mice are rescued by the introduction of *tnfr1* gene mutation (Table 1 and Fig. 2). As shown in Fig. 4, TNFR1 relays TNF-α stimulation to three separate pathways, which include the induction of apoptosis, NF-κB activation, and SAPK/JNK activation [20]. Activation of NF-κB protects against TNF-α-induced apoptosis.